Comprehensive Photophysical and Nonlinear Spectroscopic Study of Thioanisolyl-Picolinate Triazacyclononane Lanthanide Complexes

Dina Akl,[a] Lucile Bridou,[a] Maher Hojorat,[a] Guillaume Micouin,[a] Salauat R. Kiraev,[a] François Riobé,[b] Sandrine Denis-Quanquin,[a] Akos Banyasz,*[a] and Olivier Maury*[a]

[a] D. Akl, L. Bridou, Dr. M. Hojorat, Dr. G. Micouin, Dr. S. R. Kiraev, Dr. F. Riobé, Dr. S. Denis-Quanquin, Dr. A. Banyasz, Dr. O. Maury
CNRS UMR 5182, Laboratoire de Chimie
Univ Lyon, ENS de Lyon
46 Allée d'Italie, 69007 Lyon, France
E-mail: akos.banyasz@ens-lyon.fr; olivier.maury@ens-lyon.fr

[b] Dr. F. Riobé
CNRS UMR 5026, ICMCB
University of Bordeaux, Bordeaux INP
87 Avenue du Docteur Schweitzer, 33608 Pessac, France

Supporting information for this article is given via a link at the end of the document.

Abstract: Detailed photophysical studies of luminescent lanthanide complexes are presented and elaborated using a newly developed thioanisolyl-picolinate antenna and the related tacn macrocyclic ligand. The new ligand proved to sensitise Nd(III), Sm(III), Eu(III) and Yb(III) emission. Eu(III) complex showed complete energy transfer, yielding high quantum yield (44%) and brightness, while the Tb(III) analogue underwent a thermally activated back-energy transfer, resulting in a strong oxygen quenching of the triplet excited state. Transient absorption spectroscopy measurements of Gd(III), Tb(III) and Eu(III) compounds confirmed the sensitization processes upon the charge-transfer antenna excitation. The triplet excited state lifetime of the Tb(III) complex was 5-times longer than that of the Gd(III) analogue. In contrast, the triplet state was totally quenched by the energy transfer to the *4f*-metal ion in the Eu(III) species. Nonlinear two-photon absorption highlighted efficient biphotonic sensitization in Eu(III) and Sm(III) complexes. In case of the Nd(III) compound, one-photon absorption in *4f-4f* transitions was predominant, despite the excitation at the antenna two-photon band. This phenomenon was due to the Nd(III) *4f-4f* transitions overlapping with the wavelength-doubled absorption of the complex.

Introduction

The *4f*-elements luminescence is particularly attractive for biological applications, such as microscopy, biosensing and fluoroimmunoassays due to its characteristic features.[1] This luminescence arises from *4f-4f* transitions that are very sharp, characteristic of each element due to the shielding of the *4f* orbitals by the filled $5p^6$ and $5s^2$ ones and present a Laporte forbidden character. As a consequence, lanthanide(III) ions (Ln(III)) luminescence is long-lived (µs–ms) compared to endogenous fluorescence (ns) originating from organic or biological chromophores.[2] These features provide an improved signal-over-noise ratio using a time-gated detection mode.[3] The large variety of luminescent *4f*-metal ions offers a palette of emission wavelengths from UV (Gd) and visible (Eu, Tb, Sm, Dy) the near-infrared (NIR) range (Sm, Yb, Nd, Er) corresponding to the biological transparency window.[4] The chemical similarities between 13 spectroscopically active lanthanides (from Ce to Yb)[5] allow using the same organic ligands to obtain and optimize the desired Ln(III) emission via the antenna effect.[2] The latter is a process, during which an organic chromophore absorbs light and transfers the energy to the Ln(III), resulting in *4f-4f* luminescence.[6] Thus, the appropriate light-harvesting antennae should be designed and optimised to capitalise on characteristic lanthanide emission and achieve the desired photophysical properties. For practical applications, the antenna should sufficiently absorb light above 350 nm to allow excitation through the glass microscope objective and plastic sample holders,[1d] and enable two-photon (2P) excitation in the operating range of the conventional Ti:Sapphire laser sources [680–1050 nm].[7]

In this context, the design of bright lanthanide bioprobes has been extensively studied the last decades. The brightness represents the amount of light available for detection in biological applications and is defined for a linear one-photon (1P) excitation process as the product $B^1(\lambda) = \varepsilon(\lambda)\cdot\Phi$, where $\varepsilon(\lambda)$ is the molar absorption coefficient and Φ is the emission quantum yield. By analogy, the two-photon brightness is defined by $B^2(\lambda) = \sigma^2(\lambda)\cdot\Phi$, with $\sigma^2(\lambda)$ as the 2P absorption cross-section expressed in Goeppert-Mayer (GM).[7]

Among the large variety of Ln coordination compounds developed for these applications, complexes featuring charge-transfer (CT) antennae by association of electron donating fragments (*e.g.* alkoxyphenyl) to electron withdrawing motifs (*e.g.* picolinate) via conjugated backbone are particularly attractive, as they generally have very large extinction coefficients and strong 2P absorption resulting in optimal brightness.[8] In particular, the alkoxyphenyl-ethynyl-picolinate antenna was found to maximise Eu(III) brightness and is now ubiquitous in the field.[9]

As an example, **EuL^1** (Figure 1a) has strong extinction coefficients ($\varepsilon = 58 \times 10^3$ L·M^{-1}·cm^{-1}) and large lanthanide emission quantum yields ($\Phi_{Ln} = 48\%$)[9a, 10] with red-shifted absorption wavelengths up to 375 nm resulting in optimized brightness and enabling a

good compatibility for 1P and 2P microscopy.[11] Such chromophores as the antenna in **EuL^1** were combined with various azamacrocyclic platforms, such as tacn,[1e, 9a, 10, 12] pyclen,[13] cyclen,[1e, 14] DO3A,[1e, 15] cyclam[16] and other.[17] Among these complexes, the cationic Eu(III) species were found to be spontaneously internalised *in cellulo*,[14a, 17a] or used as sensors for anion analytes,[18] while neutral or anionic complexes found interesting applications as bioconjugates.[10, 15b, 15c, 19]

Why using these complexes for the above-mentioned biological applications, some unexpected drawbacks have been identified by the groups of Tripier and Sénèque: (i) the triple bond in the antenna structure is not perfectly stable and (ii) is sensitive towards cysteine-containing peptides and proteins in cellular media[15b] or it is partially destroyed in strongly acidic TFA media generally used during peptide synthesis.[13c] As an example, the alkoxyphenyl-ethynyl-picolinate complex of DO3A (**EuLc^1**, Figure 1c) underwent thiol-yne addition of the cysteine- and methionine-containing peptides.[15b]

Consequently, the following antenna generation had alkoxyphenyl donors directly conjugated to the picolinates (**EuL^2**, Figure 1a) to improve their robustness and chemical inertness.[20] The resulting *p*-anisolyl-picolinates were deprived of the triple bond, yielding equally emissive Eu-complexes as **EuL^1**, albeit with decreased absorption cut-off wavelength ($\lambda_{cut\text{-}off}$ < 350 nm),[20] below which the antenna absorbs the light.

Herein, we report lanthanide complexes of the new antenna with the thioanisolyl stronger donor replacing *p*-anisolyl to counterbalance the removal of the ethynyl bridge and red-shift the absorption spectrum (**EuL^3**, Figure 1b). Three thioanisolyl-picolinate antenna fragments were combined with the tacn macrocycle encapsulating visible (Ln = Eu, Tb, Sm) and NIR (Ln = Sm, Nd, Yb) emitting Ln(III) in the nonadentate coordination environment. Their photophysical properties were studied via 1P and 2P fluorescence spectroscopy techniques and transient absorption. All synthesised complexes had appropriate absorption values at $\lambda_{cut\text{-}off}$ = 370 nm, and the Eu(III) emission quantum yield was as large (Φ_{Ln} = 44%) as the previous generation of CT antenna compounds. Thus, the modification of antenna structure with sulphur proved to be a viable strategy to reinforce the aryl donor and, as a consequence, to bathochromically shift the absorption spectrum while preserving the CT sensitising effect for the bright lanthanide emission.

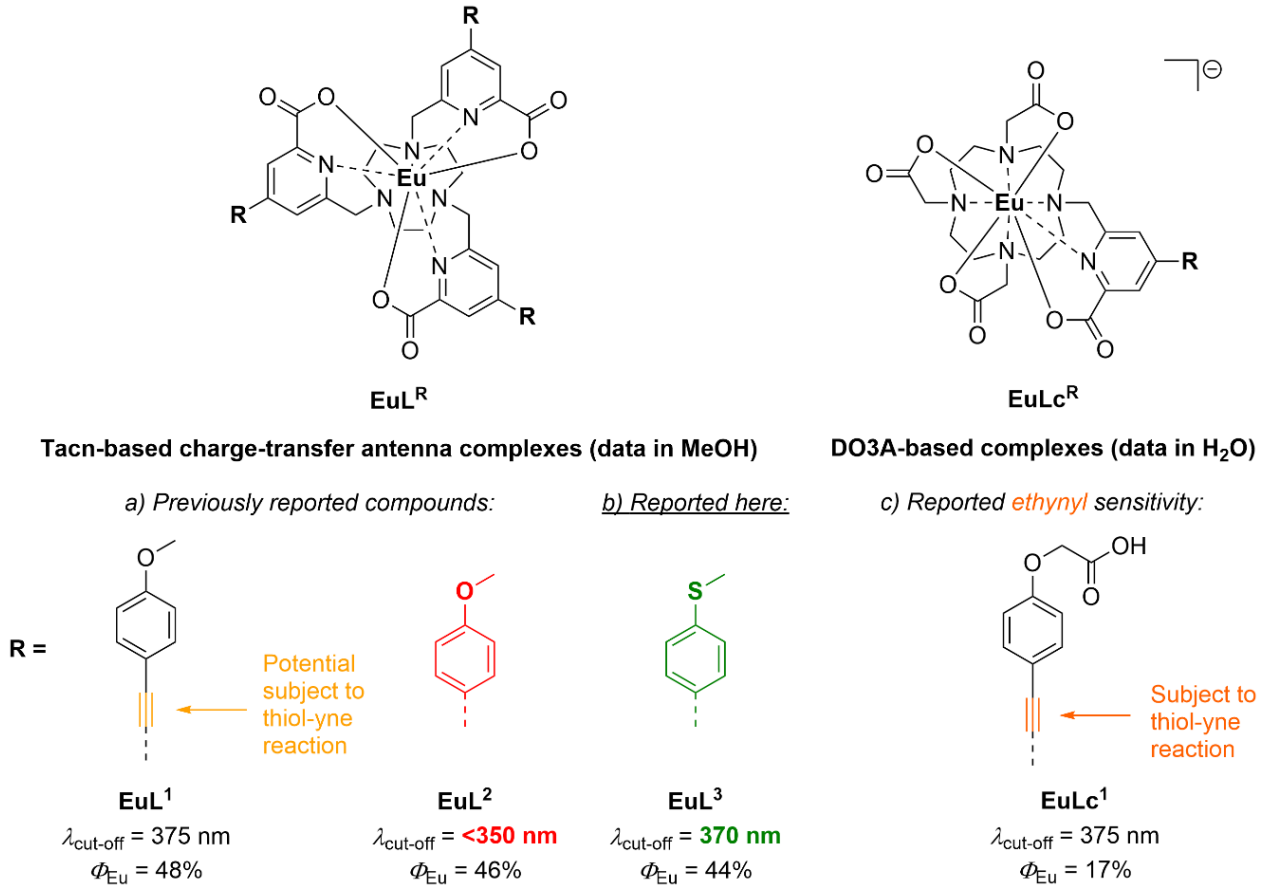

Figure 1. Top: structures of Eu complexes with trispicolinate-tacn (left, **EuL^R**) and picolinate-DO3A (right, **EuLc^R**) ligand platforms functionalised by the selected CT antenna donors (**R**, bottom) in the picolinate *p*-positions; a) Previously reported *p*-anisolyl-ethynyl (left, **EuL^1**) and *p*-anisolyl (right; **EuL^2**) CT antenna donors; b) **EuL^3** reported here with thioanisolyl donor groups; c) Reported sensitivity of ethynyl-containing donor group to thiol-yne reaction (**EuLc^1**).

Results and Discussion

Synthesis and Characterisation

The synthetic pathway to prepare the new antenna (**4**), the tacn-incorporated ligand (**L3'**) and its corresponding lanthanide complexes (**LnL^3**) is depicted in Figure 2. The synthesis of the thioanisolyl-dipicolinate antenna (**4**) commenced from the Miyaura borylation of 4-bromothioanisole (**1**) with bis(pinacolato)diboron in excellent 90% yield. The obtained boronic ester (**2**) was coupled to dimethyl 4-iododipicolinate (**3**) in a Suzuki-Miyaura reaction, yielding the target antenna (**4**, 84%). The diester **4** was monoreduced by sodium borohydride in a methanol:dichloromethane 1:2 mixture, affording the corresponding alcohol **5** in 80% yield. The monoalcohol **5** was activated by mesylation with triethylamine as a base in dichloromethane (**6**, quant.) and was used for the trialkylation of tacn trihydrochloride (**7**) in the presence of excess sodium carbonate in acetonitrile. The tris-substituted tacn **L$^{3'}$** was isolated in 73% yield after column chromatography on alumina. After saponification, the deprotected ligand was complexed with $LnCl_3{\cdot}6H_2O$ forming the target lanthanide compounds **LnL^3** in high yields (70–93%, Ln = Nd, Sm, Eu, Gd, Tb, Yb and Lu).

The reaction products were purified by the column chromatography on silica gel (**2**–**6**) or activated alumina (**L$^{3'}$**). The structures of the prepared compounds were unambiguously confirmed by NMR and HRMS analyses (see the supporting information). The complete conversion of **L$^{3'}$** to the corresponding lanthanide complexes **LnL^3** was monitored by FT-IR spectroscopy (Figures S1–8). The C=O vibrational transitions in **L$^{3'}$** at 1717–1738 cm^{-1} shifted to lower energies at 1634–1641 cm^{-1} in **LnL^3** upon the deprotection of methyl groups. Thus, the absence of the methyl ester C=O vibrations in the FT-IR spectra of **LnL^3** indicated the purity of the final lanthanide complexes.

To investigate the structural composition of **LnL^3** complexes, we performed diamagnetic (Ln = Lu) and paramagnetic (Ln = Eu, Yb) NMR spectroscopy characterisation in DMSO-d^6 solutions. The spectra and their assignment are in SI (Figures S9–19). The ^{1}H chemical shifts of diamagnetic **LuL^3** species were fully assigned with the help of 2D NMR spectra (Figure S14). The paramagnetic Eu(III) and Yb(III) complexes spectra were also well-resolved and confirmed the isostructural character with **LuL^3** in solution (Figures S17,19).[21]

Photophysical Properties

All the photophysical measurements were performed in spectroscopic grade solvents (MeOH or CH_2Cl_2) with μM concentrations of the complexes. The absorption spectra of **LnL^3** compounds had similar profiles with a broad structureless band assigned to the CT transition and the local maxima centred at 328–331 nm (Figures 3, 4, S20). This $S_0 \rightarrow S_1$ transition was independent of the Ln(III) nature,[22] ensuring the involvement of the same antenna excited states in the sensitisation of the *4f*-emission. The more electron-rich thioether donor red-shifted the **EuL^3** absorption compared to that of the methoxy-substituted analogue **EuL^2** ($\Delta\lambda^3$ = 18 nm, Figure S21). This functionalisation had an almost similar effect as the addition of the ethynyl bridge in **EuL^1**, which gave an extra bathochromic shift due to extended π-conjugated system ($\Delta\lambda^1$ = 26 nm=.

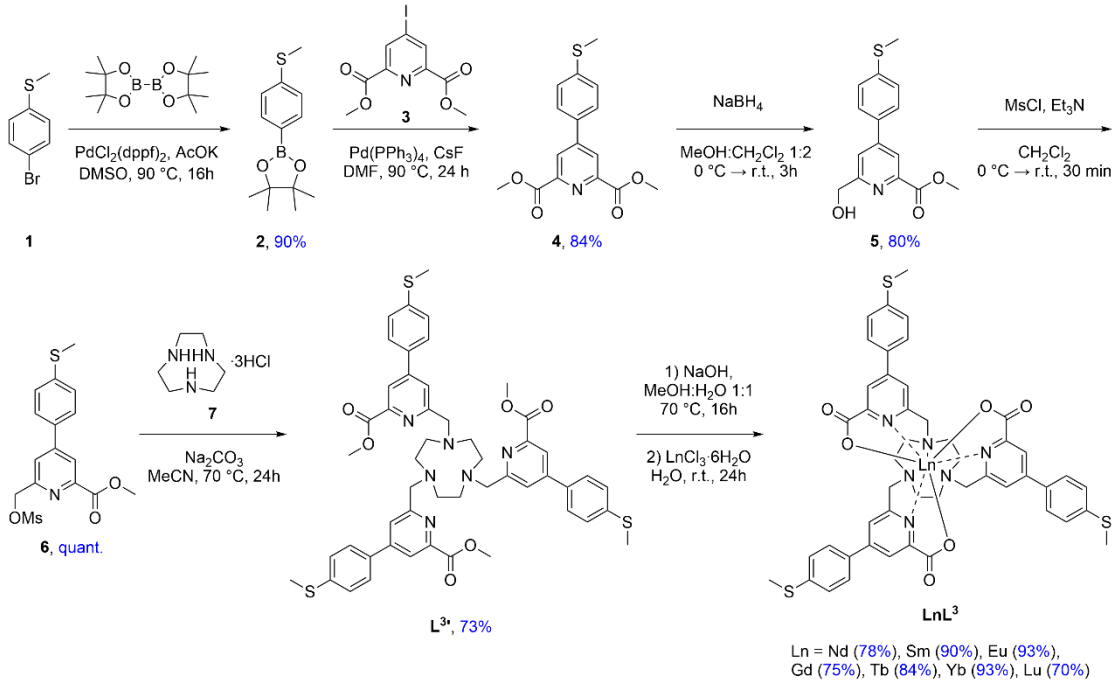

Figure 2. Synthesis of the new thioanisolyl-dipicolinate antenna **4**, the tacn-based protected ligand **L$^{3'}$** and the final Ln complexes **LnL^3**.

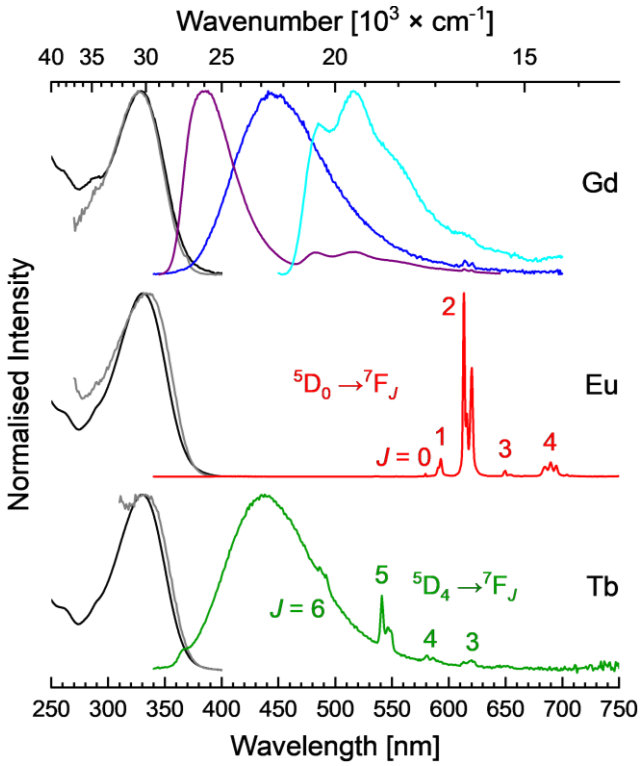

Figure 3. Normalised absorption (black), excitation (grey, λ_{em} = 415 nm for Gd, 613 nm for Eu and 541 nm for Tb) and emission spectra of **LnL³** complexes (Ln = Eu, Gd, Tb, [**LnL³**] ≈ 1–2 μM) in MeOH in aerated conditions (λ_{exc} = 328 or 330 nm, Gd: blue at 293 K, purple at 77 K, cyan at 77 K after 0.05 ms delay; Eu: red; Tb: green). **GdL³** spectra at 77 K were measured in EtOH:MeOH (4:1).

The CT energy level of the antenna in the **LnL³** complexes was estimated from the intersection of the **GdL³** complex absorption and emission spectra at 293 K,[23] E_{CT} = 26700 cm^{-1}. We measured the steady-state and time-resolved emission spectra of **GdL³** at 77 K in EtOH:MeOH (4:1) glass to estimate the triplet energy level of the sensitising antenna. In the steady-state conditions, both CT and triplet state emissions were observed. The ligand phosphorescence was recorded after 0.05 ms delay, revealing the triplet excited state (T_1) at 20600 cm^{-1}. Finally, the phosphorescence decay was measured for **GdL³** at 77 K providing a triplet lifetime value of 21 ms (Figure S23). Hence, the T_1 energy level was significantly higher than the excited states of Eu(III) ($^5D_0$, 17300 cm^{-1}), Sm(III) ($^4G_{5/2}$, 17900 cm^{-1}), Yb(III) ($^2F_{5/2}$, 10300 cm^{-1}) and Nd(III) ($^4F_{3/2}$, 11600 cm^{-1}).[24] The $^5D_4$ (20500 cm^{-1}) receiving level of Tb(III) and the antenna triplet had the same energies, which could stimulate back energy transfer process.

Upon excitation in the CT band, the characteristic Eu(III) emission spectrum was observed without any residual ligand-centred CT fluorescence indicating a complete energy transfer. The emission profile of **EuL³** was identical to that of the **EuL²** and **EuL¹** analogues,[9a, 20] with $^5D_0 \rightarrow {}^7F_J$ transitions at 580 nm (J = 0), 594 nm (J = 1), 614 nm (J = 2), 650 nm (J = 3) and 691 nm (J = 4, Figure 3 and S21). The intensity ratio is characteristic of a D_3 symmetric complex with a least intense ΔJ = 0 band and ΔJ = 2 accounting for more than 80% of the total luminescence.

Table 1. Photophysical properties of **LnL³** complexes in MeOH. λ_{max} – first absorption maximum of the ligand; ε – molar extinction coefficient; Φ - emission quantum yields, respectively; τ – lifetime.

Complex	λ_{max} [nm]	ε [a]	Φ [%] [b]	τ [μs] [c]
NdL³	328	46	/	0.27
SmL³	331	44	0.35 [d]	28
EuL³	330	57	44	965
GdL³	330	50	4.7	/
TbL³	330	49	1.6 [e]	<20 [f]
YbL³	329	45	/	5.2
LuL³	329	51	/	/

[a] In 10^3 L·M^{-1}·cm^{-1}. [b] Measured using quinine bisulfate as a reference (1 *N* H_2SO_4, Φ_{ref} = 54.6%)[25] at λ_{exc} = 328, 330 or 331 nm. [c] Measured using λ_{exc} = 330 or 331 nm and λ_{em} = 1060 nm (Nd), 650 nm (Sm), 614 nm (Eu), 541 nm (Tb), 970 nm (Yb). [d] Only for the visible part of the emission 553–750 nm. [e] Calculated including the Tb emission. [f] The lifetime was too small to be measured with the μs flash lamp (7 μs pulse duration).

The **EuL³** lanthanide emission quantum yield was 44% (Table 1), which was similar to the values of the previously studied complexes with *p*-anisolyl- and *p*-anisolyl-ethynyl-picolinate antennae. In combination with the large extinction coefficient (ε = 58 × 10^3 L·M^{-1}·cm^{-1}, Table 2), the thioanisolyl-picolinate antenna-sensitised **EuL³** complex makes up 25 × 10^3 L·M^{-1}·cm^{-1} brightness in MeOH ($B^1(\lambda)$, see introduction). This value is in the same range as the brightness of the **EuL¹** complex sensitised by the first *p*-alkoxyphenyl-ethynyl-picolinate antenna generation. However, the absorption of **EuL³** is more suitable for microscopy and 2P excitation requirements (*vide supra*) than that of the **EuL²** complex without the triple bond conjugation.

Table 2. Comparison of Eu photophysical properties in MeOH in the series of complexes with tacn ligands sensitised by picolinate antennae with *p*-anisolyl-ethynyl (**L¹**), *p*-anisolyl (**L²**) or thioanisolyl (**L³**) donor groups.

Complex	$\lambda_{cut\text{-}off}$ [nm]	λ_{max} [nm]	ε [a]	Φ [%] [b]	$B^1(\lambda)$ [a]
EuL¹ [c]	375	338	58	48	28
EuL²	350	312	52	46 [d]	24
EuL³	370	330	57	44	25

[a] In 10^3 L·M^{-1}·cm^{-1}. [b] Measured using quinine bisulfate as a reference (1 *N* H_2SO_4, Φ_{ref} = 54.6%).[25] [c] From the reference.[1] [d] From the reference.[17]

In marked contrast, the emission spectrum of **TbL³** (Figure 3) was dominated by the ligand-centred emission, with the characteristic

Tb(III) $^5D_4 \rightarrow {}^7F_J$ (J = 6–3) transitions being only detected in the red-tail of the fluorescence band. Under these conditions, the Tb(III) emission quantum yield was not measured and the lifetime was too short to be detected with our set-up. The ligand-centred emission quantum yield of the Tb complex was 1.6%, which was 3-fold smaller than the **GdL³** value (Φ = 4.7%, Table 1). These data strongly suggested that a very efficient thermally activated back-energy transfer occurred from the Tb(III) excited state to the energetically close-lying ligand triplet. To confirm this hypothesis, photophysical measurements were performed in degassed medium (Figure S25) or at low temperature (77 K, Figure S26). In both cases, Tb(III) emission was significantly increased in intensity and lifetime, validating this hypothesis.

To get a further insight into the sensitization process, transient absorption spectroscopy (TAS) was performed in degassed methanol solutions (Figure 4). In the case of **GdL³**, a well-resolved triplet-triplet excited state absorption was observed, centred at 530 nm with a lifetime of 1.7 µs (this lifetime was only 0.4 µs in aerated solution due to oxygen quenching, further confirming the assignment of the band to a triplet state). Replacing Gd by Eu resulted in a straightforward *4f*-luminescence sensitization with the absence of any residual ligand-centred emission. The energy transfer from the ligand to the *4f*-metal in **EuL³** was total and very rapid, thus it was impossible to detect any triplet absorption using TAS. In the case of the Tb-complex, TAS revealed the same ligand-centred triplet-triplet absorption band as for the Gd-complex. The main difference was the 5-fold longer triplet lifetime (8.5 µs) of the Tb-complex than that of the **GdL³** (Figure 4). Such an increase of the ligand-centred triplet excited state lifetime is perfectly in line with the back energy transfer from Tb(III) to the ligand (*vide infra*). As a result, the triplet excited state is in equilibrium with a long-lived (150 µs) Tb-centred $^5D_4$ level increasing the triplet lifetime in **TbL³**.

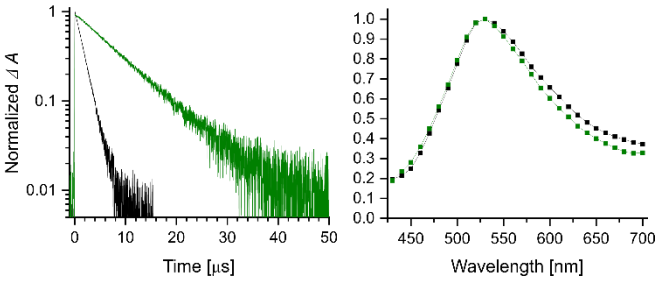

Figure 4. Gd (black) and **TbL³** (green) transient absorption decays observed at 530 nm (left) and transient absorption spectra obtained at 0.15 and 0.4 µs delay after the excitation, respectively (right). [**GdL³**] = 5.1 µM and [**TbL³**] = 3.8 µM in MeOH, λ_{exc} = 355 nm. The vertical scales for both spectra are in normalised ΔA.

LnL³ complexes with NIR emitting lanthanides (Ln = Sm, Yb and Nd) had demonstrated *4f*-luminescence in the expected regions (Figure 5, Table 1) with the reasonable emission lifetimes similar to the reported values in the literature for the analogical coordination environments.[12a, 12c] Along with *4f*-metal-centred emissions, ligand fluorescence was also observed. **SmL³** is the only dual emitter in the series, with transitions both in the visible (Φ_{Ln} = 0.35%) and NIR range. Thus, the new thioanisolyl-picolinate is a versatile antenna able to sensitise the emission of several different lanthanide ions.

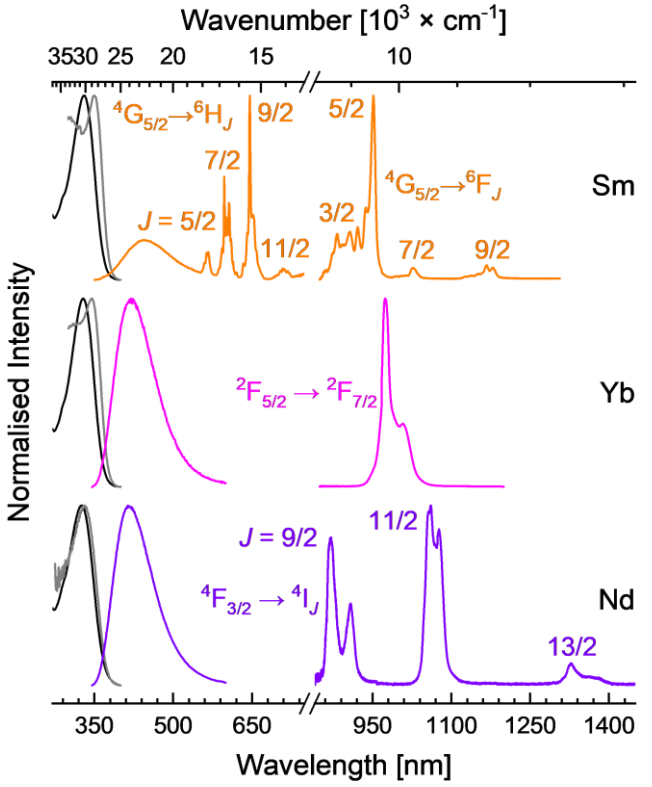

Figure 5. Normalised absorption (black), excitation (grey, λ_{em} = 645 nm for Sm, 976 nm for Yb and 1059 nm for Nd) and emission (λ_{exc} = 331 nm, Sm: orange; Yb: magenta, Nd: violet) spectra of **LnL³** complexes (Ln = Sm, Yb, Nd, [**LnL³**] ≈ 1–2 µM) in MeOH.

Two-photon absorption properties

The two-photon absorption properties of the Sm, Eu and Nd(III) complexes were measured in methanol using our in-house optical set-up equipped with a fs-Ti:Sapphire laser source. For all studied complexes upon excitation between 680-810 nm, the characteristic *4f*-element luminescence was observed. In the case of **EuL³** and **SmL³**, the variation of the luminescence intensity displayed quadratic dependence with the incident average laser power (Figure 6, experimental slope of 1.96 and 1.90 for Sm and Eu, respectively). This quadratic dependence is the clear signature of the lanthanide sensitization by a two-photon antenna effect from the conjugated ligand. The two-photon absorption cross-section, σ^2, was determined using fluorescein as an external standard in the case of the most emissive **EuL³** complex. As expected for a non-centrosymmetric complex, the spectra of 2P excitation and the wavelength-doubled 1P absorption overlapped accordingly (Figure 7), indicating the low-lying CT state is responsible for the Eu(III) sensitization. The maximal σ^2 value is 50 GM at 680 nm which is in the classical range for such antenna. Due to spectral limitation of the incident

laser source (> 680 nm), the maximum of the two-photon absorption band could not be reached.

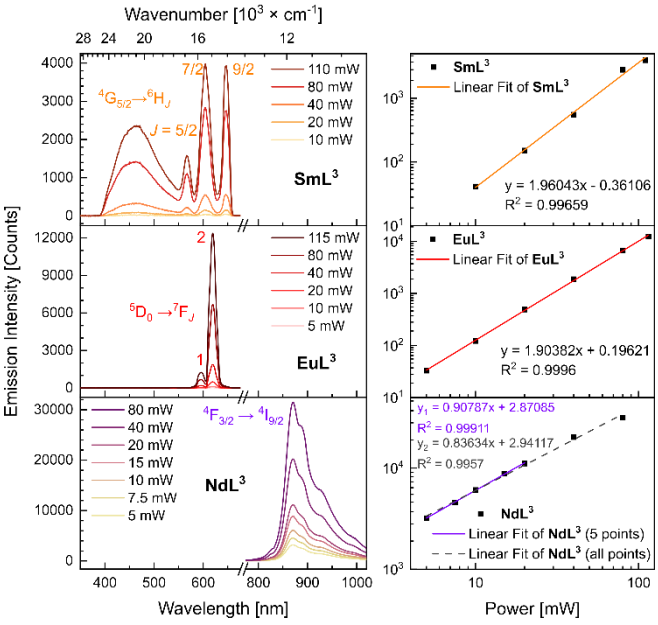

Figure 6. Left: 2P (Ln = Sm, Eu; in MeOH) and 1P (Ln = Nd; in CH_2Cl_2) emission spectra of **LnL³** complexes. Right: plots of the Sm, Eu and Nd emission intensities at 640, 620 and 871 nm versus incident average laser power for **Sm**, **Eu** and **NdL³** on a log/log scale. The fits of the experimental data (shown in black scatter) are shown as coloured lines, fitted model function, the obtained parameters and standard deviations are reported in insets. The scales on the right plots represent emission intensity [counts] as on the left emission spectra, λ_{exc} = 700 (Sm, Nd) or 710 (Eu) nm, **[SmL³] = [NdL³]** = 10 µM, **[EuL³]** = 3.2 µM.

The case of **NdL³** was particular, as a linear dependence of the luminescence intensity versus the incident laser power was observed (followed by a slight saturation effect at higher laser power), signifying a dominant 1P excitation process. This phenomenon was rationalized by the *4f-4f* absorption band in this range and especially the $^4I_{9/2} \rightarrow {}^4F_{7/2}$ (740 nm) and $^4I_{9/2} \rightarrow {}^2H_{9/2}$ (800 nm) transitions.[24, 26] Despite the forbidden nature of the *4f-4f* transitions for 1P excitation, they were still more probable than the nonlinear 2P absorption in the CT antenna and completely masked its contribution to the sensitisation of the Nd(III) emission. Our attempts to circumvent this problem by shifting the excitation wavelength to 700 nm (at higher energies than the *4f-4f* transitions) still yielded the Nd(III)-based 1P excitation, as the spectral dispersion of the laser overlapped with the *4f-4f* absorption. This indicated that the one-photon excitation of the *4f-4f* transition was the ultra-dominant process. Hence, the only way to sensitize Nd(III) emission by a two-photon absorption process is to shift the excitation in the NIR above 1000 nm requiring the design of a more conjugated CT antenna.

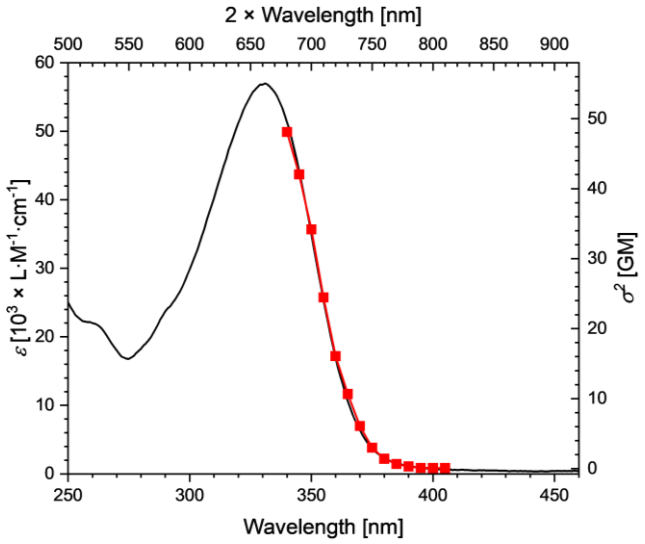

Figure 7. Two-photon excitation (red line and scatter) and one-photon absorption (black line) spectra of **EuL³** in MeOH, **[EuL³]** = 3.2 µM. The bottom and top scales correspond to the wavelength of one- and two-photon spectra, respectively.

Conclusion

We report the synthesis of a new thioanisolyl-picolinate charge-transfer antenna and the photophysical properties of the tacn-incorporated lanthanide complexes with Ln(III) = Nd, Sm, Eu, Gd, Tb, Yb and Lu. The complexes solution structures revealed the presence of single species according to diamagnetic (Lu) and paramagnetic (Eu and Yb) NMR spectroscopic analysis. Very different photophysical behaviour was observed depending on the nature of the *4f*-element in the complex. In the case of Eu(III), the energy transfer was complete, resulting in 44% quantum yield and 25×10^3 $L \cdot M^{-1} \cdot cm^{-1}$ brightness, being among the highest values described for this element in the literature. For NIR (Nd, Yb) and dual vis-NIR emitters (Sm) the transfer was not optimal, but the sensitisation of the lanthanide luminescence was still successful. In the case of Tb, a back-energy transfer was evidenced, almost completely quenching the green luminescence. In addition, the use of transient absorption spectroscopy appears to be particularly useful to investigate the sensitisation mechanisms and the non-radiative processes. In our case, the triplet lifetime was 5-times longer in the Tb complex upon the triplet repopulation than in Gd species. Finally, the nonlinear two-photon absorption properties were investigated, demonstrating efficient two-photon-sensitization process in Eu and Sm(III) complexes. However, the Nd(III) analogue underwent one-photon absorption in *4f-4f* transitions when using the two-photon excitation wavelength for the CT antenna sensitisation. In conclusion, the thioanisolyl-picolinate antenna appears as a versatile and promising chromophore for the design of useful lanthanide luminescent probes for biological applications considering the water solubility and bioconjugation issues. The research is ongoing in our group to resolve the latter challenges.

Supporting Information

The authors have cited additional references within the Supporting Information.[27–32]

Acknowledgements

Authors acknowledge the Agence Nationale de la Recherche (ANR-21-CE29-0018 and ANR-21-CE07-0063) and Aviesan ITMO Cancer PCSI program (ONCOVIEW project) for financial support. Authors thank Yannick Guyot (ILM Lyon) for measuring the NIR lifetimes. The authors also acknowledge Yann Bretonnière (ENS Lyon), Olivier Sénèque (CEA Grenoble), Raphaël Tripier (Unviersity of Brest) and Eric Kennehan (Magnitude Instruments) for fruitful discussions.

Keywords: Lanthanide luminescence • antenna • macrocycle • transient absorption spectroscopy • two-photon absorption

References

[1] a) A. G. Cosby, K. E. Martin, E. Boros, in *Modern Applications of Lanthanide Luminescence* (Ed.: A. de Bettencourt-Dias), Springer International Publishing, Cham, **2023**, 175-194; b) M. Sy, A. Nonat, N. Hildebrandt, L. J. Charbonniere, *Chem. Commun.* **2016**, *52*, 5080-5095; c) M. C. Heffern, L. M. Matosziuk, T. J. Meade, *Chem. Rev.* **2014**, *114*, 4496-4539; d) S. V. Eliseeva, J. C. Bunzli, *Chem. Soc. Rev.* **2010**, *39*, 189-227; e) D. Parker, J. D. Fradgley, K.-L. Wong, *Chem. Soc. Rev.* **2021**, *50*, 8193-8213. f) S. E. Bodman, S. J. Butler *Chem. Sci.*, **2021**, 12, 2716–2734

[2] J.-C. G. Bünzli, S. V. Eliseeva, in *Lanthanide Luminescence: Photophysical, Analytical and Biological Aspects* (Eds.: P. Hänninen, H. Härmä), Springer Berlin Heidelberg, Berlin, Heidelberg, **2011**, 1-45.

[3] E. Mathieu, A. Sipos, E. Demeyere, D. Phipps, D. Sakaveli, K. E. Borbas, *Chem. Commun.* **2018**, *54*, 10021-10035.

[4] J. C. G. Bünzli, S. V. Eliseeva, in *Comprehensive Inorganic Chemistry II (Second Edition)* (Eds.: J. Reedijk, K. Poeppelmeier), Elsevier, Amsterdam, **2013**, 339-398.

[5] A. de Bettencourt-Dias, in *Luminescence of Lanthanide Ions in Coordination Compounds and Nanomaterials*, **2014**, 1-48.

[6] S. I. Weissman, *J. Chem. Phys.* **1942**, *10*, 214-217.

[7] A. D'Aléo, C. Andraud, O. Maury, in *Luminescence of Lanthanide Ions in Coordination Compounds and Nanomaterials*, **2014**, 197-230.

[8] A. D'Aléo, F. Pointillart, L. Ouahab, C. Andraud, O. Maury, *Coord. Chem. Rev.* **2012**, *256*, 1604-1620.

[9] a) J. W. Walton, A. Bourdolle, S. J. Butler, M. Soulie, M. Delbianco, B. K. McMahon, R. Pal, H. Puschmann, J. M. Zwier, L. Lamarque, O. Maury, C. Andraud, D. Parker, *Chem. Commun.* **2013**, *49*, 1600-1602; b) S. J. Butler, M. Delbianco, L. Lamarque, B. K. McMahon, E. R. Neil, R. Pal, D. Parker, J. W. Walton, J. M. Zwier, *Dalton Trans* **2015**, *44*, 4791-4803.

[10] V. Placide, A. T. Bui, A. Grichine, A. Duperray, D. Pitrat, C. Andraud, O. Maury, *Dalton Trans.* **2015**, *44*, 4918-4924.

[11] a) A. D'Aléo, A. Picot, P. L. Baldeck, C. Andraud, O. Maury, *Inorg. Chem.* **2008**, *47*, 10269-10279; b) A. D'Aléo, A. Picot, A. Beeby, J. A. Gareth Williams, B. Le Guennic, C. Andraud, O. Maury, *Inorg. Chem.* **2008**, *47*, 10258-10268.

[12] a) A. D'Aléo, A. Bourdolle, S. Brustlein, T. Fauquier, A. Grichine, A. Duperray, P. L. Baldeck, C. Andraud, S. Brasselet, O. Maury, *Angew. Chem. Int. Ed.* **2012**, *51*, 6622-6625; b) M. Soulié, F. Latzko, E. Bourrier, V. Placide, S. J. Butler, R. Pal, J. W. Walton, P. L. Baldeck , B. Le Guennic, C. Andraud, J. M. Zwier, L. Lamarque, D. Parker, O. Maury, *Chem. Eur. J.* **2014**, *20*, 8636-8646; c) A. T. Bui, A. Grichine, S. Brasselet, A. Duperray, C. Andraud, O. Maury, *Chem. Eur. J.* **2015**, *21*, 17757-17761; d) E. R. Neil, M. A. Fox, R. Pal, L.-O. Palsson, B. A. O'Sullivan and D. Parker*, Dalton Trans*., **2015**, *44*, 14937–14951..

[13] a) N. Hamon, M. Galland, M. Le Fur, A. Roux, A. Duperray, A. Grichine, C. Andraud, B. Le Guennic, M. Beyler, O. Maury, R. Tripier, *Chem. Commun.* **2018**, *54*, 6173-6176; b) N. Hamon, A. Roux, M. Beyler, J.-C. Mulatier, C. Andraud, C. Nguyen, M. Maynadier, N. Bettache, A. Duperray, A. Grichine, S. Brasselet, M. Gary-Bobo, O. Maury, R. Tripier, *J. Am. Chem. Soc.* **2020**, *142*, 10184-10197; c) N. Hamon, L. Bridou, M. Roux, O. Maury, R. Tripier, M. Beyler, *J. Org. Chem.* **2023**, *88*, 8286-8299.

[14] a) A. T. Bui, M. Beyler, Y.-Y. Liao, A. Grichine, A. Duperray, J.-C. Mulatier, B. L. Guennic, C. Andraud, O. Maury, R. Tripier, *Inorg. Chem.* **2016**, *55*, 7020-7025; b) L. B. Jennings, S. Shuvaev, M. A. Fox, R. Pal, D. Parker *Dalton Trans.* **2018**, *47*, 16145-16154.

[15] a) A. D'Aléo, M. Allali, A. Picot, P. L. Baldeck, L. Toupet, C. Andraud, O. Maury, *C. R. Chimie* **2010**, *13*, 681-690; b) J.-H. Choi, G. Fremy, T. Charnay, N. Fayad, J. Pécaut, S. Erbek, N. Hildebrandt, V. Martel-Frachet, A. Grichine, O. Sénèque, *Inorg. Chem.* **2022**, *61*, 20674-20689; c) Y. Zhang, X. Ma, H.-F. Chau, W. Thor, L. Jiang, S. Zha, W.-Y. Fok, H.-N. Mak, J. Zhang, J. Cai, C.-F. Ng, H. Li, D. Parker, L. Li, G.-L. Law, K.-L. Wong, *ACS Appl. Nano Mater.* **2021**, *4*, 271-278.

[16] J. Mendy, A. Thy Bui, A. Roux, J.-C. Mulatier, D. Curton, A. Duperray, A. Grichine, Y. Guyot, S. Brasselet, F. Riobé, C. Andraud, B. Le Guennic, V. Patinec, P. R. Tripier, M. Beyler, O. Maury, *ChemPhysChem* **2020**, *21*, 1036-1043.

[17] a) A. Bourdolle, M. Allali, J.-C. Mulatier, B. Le Guennic, J. M. Zwier, P. L. Baldeck, J.-C. G. Bünzli, C. Andraud, L. Lamarque, O. Maury, *Inorg. Chem.* **2011**, *50*, 4987-4999; b) M. Schäferling, T. Aaritalo, T. Soukka, *Chem.–Eur. J.*, **2014**, *20*, 5298–5308S. c) H. Sund, Y. Y. Liao, C. Andraud, A. Duperray, A. Grichine, B. Le Guennic, F. Riobe, H. Takalo, O. Maury, *ChemPhysChem* **2018**. d) Mizzoni, S. Ruggieri, A. Sickinger, F. Riobé, L. Guy, M. Roux, G. Micouin, A. Banyasz, O. Maury, B. Baguenard, A. Bensalah-Ledoux, S. Guy, A. Grichine, X.-N. Nguyen, A. Cimarelli, M. Sanadar, A. Melchior, F. Piccinelli, *J. Mater. Chem. C* **2023**, *11*, 4188-4202;

[18] S. J. Butler, B. K. McMahon, R. Pal, D. Parker, J. W. Walton, *Chem. Eur. J.* **2013**, *19*, 9511-9517.

[19] R. Lengacher, K. E. Martin, D. Smilowicz, H. Esseln, P. Lotlikar, A. Grichine, O. Maury, E. Boros, *J. Am. Chem. Soc.* **2023**, *145*, 24358-24366.

[20] A. T. Bui, A. Grichine, A. Duperray, P. Lidon, F. Riobé, C. Andraud, O. Maury, *J. Am. Chem. Soc.* **2017**, *139*, 7693-7696.

[21] a) G. Nocton, A. Nonat, C. Gateau, M. Mazzanti, *Helv. Chim. Acta* **2009**, *92*, 2257-2273; b) J. W. Walton, R. Carr, N. H. Evans, A. M. Funk, A. M. Kenwright, D. Parker, D. S. Yufit, M. Botta, S. De Pinto, K.-L. Wong, *Inorg. Chem.* **2012**, *51*, 8042-8056; c) S. R. Kiraev, E. Mathieu, D. Kovacs, J. A. L. Wells, M. Tomar, J. Andres, K. E. Borbas, *Dalton Trans.* **2022**, *51*, 16596-16604; d) K. Mason, A. C. Harnden, C. W. Patrick, A. W. J. Poh, A. S. Batsanov, E. A. Suturina, M. Vonci, E. J. L. McInnes, N. F. Chilton, D. Parker, *Chem Commun* **2018**, *54*, 8486-8489.

[22] K. Sénéchal-David, A. Hemeryck, N. Tancrez, L. Toupet, J. A. G. Williams, I. Ledoux, J. Zyss, A. Boucekkine, J.-P. Guégan, H. Le Bozec, O. Maury, *J. Am. Chem. Soc.* **2006**, *128*, 12243-12255.

[23] G. Angulo, G. Grampp, A. Rosspeintner, *Spectrochimica Acta Part A: Molecular and Biomolecular Spectroscopy* **2006**, *65*, 727-731.

[24] W. T. Carnall, G. L. Goodman, K. Rajnak, R. S. Rana, *J. Chem. Phys.* **1989**, *90*, 3443-3457.

[25] W. H. Melhuish, *J. Phys. Chem.* **1961**, *65*, 229-235.

[26] A. Bourdolle, M. Allali, A. D'Aléo, P. L. Baldeck, K. Kamada, J. A. G. Williams, H. Le Bozec, C. Andraud, O. Maury, *ChemPhysChem* **2013**, *14*, 3361-3367.
[27] D. Montagner, V. Gandin, C. Marzano, A. Erxleben, *Eur. J. Inorg. Chem.* **2014**, *2014*, 4084-4092.
[28] A. Picot, C. Feuvrie, C. Barsu, F. Malvolti, B. Le Guennic, H. Le Bozec, C. Andraud, L. Toupet, O. Maury, *Tetrahedron* **2008**, *64*, 399-411.
[29] K.-L. Wong, J.-C. G. Bünzli, P. A. Tanner, *J. Lumin.* **2020**, *224*, 117256.
[30] Y. Arakawa, S. Kang, H. Tsuji, J. Watanabe, G.-i. Konishi, *RSC Adv.* **2016**, *6*, 92845-92851.
[31] Y. Zheng, P. Duan, Y. Zhou, C. Li, D. Zhou, Y. Wang, L.-C. Chen, Z. Zhu, X. Li, J. Bai, K. Qu, T. Gao, J. Shi, J. Liu, Q.-C. Zhang, Z.-N. Chen, W. Hong, *Angew. Chem. Int. Ed.* **2022**, *61*, e202210097.
[32] A. C. Harnden, D. Parker, N. J. Rogers, *Coord. Chem. Rev.* **2019**, *383*, 30-42.

Entry for the Table of Contents

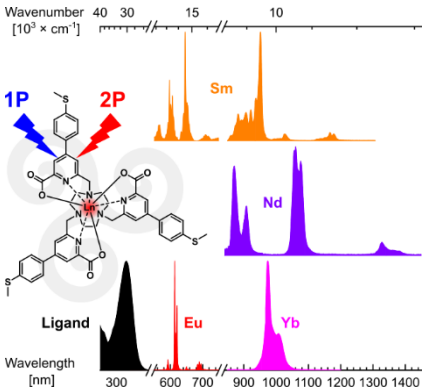

Three thioanisolyl-picolinates were incorporated with tacn in a joint macrocyclic ligand sensitising visible Eu(III) emission with 44% quantum yield, near-infrared Yb(III) and Nd(III), and dual vis-NIR Sm(III) luminescence. Eu(III) and Sm(III) emission was achieved via one- (1P, at 330 nm) and two-photon (2P, at 640–710 nm) excitation.

Institute and/or researcher Twitter usernames: @oliviermaury3, @LcEnsl